Featured in Physics

# Negative vacuum friction in terahertz gain systems

Lixin Ge*

*School of Physics and Electronic Engineering, Xinyang Normal University, Xinyang 464000, China*

(Received 17 May 2023; accepted 31 May 2023; published 14 July 2023)

Two objects in relative motion without physical contact suffer a friction force, resulting from vacuum fluctuation. It is widely accepted that friction acts in the opposite direction of the relative velocity. Here, this study demonstrates the existence of negative friction, where the direction of friction is along the sliding direction, in a gain system. The system consists of a vacuum-separated silica sphere and a dielectric substrate covered by a graphene sheet (gain medium). The friction torque of the rotating sphere can be switched between positive and negative, depending on the quasi-Fermi energy of graphene. Negative vacuum friction can be achieved when the quasi-Fermi energy is large, and its magnitude is strongly dependent on the distance, temperature, and permittivity of the substrate. For moderate conditions, the torque generated by negative friction surpasses the resistance posed by the surrounding air, presenting a different approach for driving nanoparticles to an ultrahigh rotating speed.

DOI: 10.1103/PhysRevB.108.045406

## I. INTRODUCTION

Quantum vacuum friction, an intriguing force that manifests between two objects in relative motion without physical contact, has received considerably interest [1–4]. Physically, this noncontact friction arises from the fluctuating fields contributed by the zero-point energy fluctuation and thermal electromagnetic fluctuation. The radiation of the fluctuated field undergoes a Doppler phenomenon for sliding objects, resulting in vacuum friction even at absolute zero temperature [5]. In addition to translational motions [5–8], quantum vacuum frictions in rotating micro/nanoparticles were also reported [9–15]. As an analog of the bearings in mechanical systems, rotational objects suspended in a vacuum are hindered by friction torque [13]. As the rotating nanoparticles are close to a planar substrate, the friction torque undergoes a substantial amplification with several orders of magnitude [14,15]. The enhancement is attributed to the excitation of surface plasmon polaritons (SPPs) [14] or surface phonon polaritons (SPhPs) [14,15], where a high local density of states (LDOS) is supported in close proximity to the interface. Recent advancements in experimental techniques have facilitated the levitation and rotation of nanoparticles to GHz [16–21], even with a submicrometer separation from the substrate [22], thereby opening up exciting possibilities for detecting quantum vacuum friction with heightened sensitivity.

During the friction process, the mechanical energy is largely converted into other types of energy (such as thermal energy, electrical energy, chemical energy, etc.). Dynamic friction, acting opposite to the relative velocity, inherently impedes motion. Consequently, a natural question arises: Can there exist a phenomenon of negative friction, wherein an object experiences friction along its relative sliding direction? Evidently, the negative friction within a closed system would contravene the laws of thermodynamics, as it would spontaneously accelerate the objects. Therefore, gaining energy from the outside system could be a precondition for negative friction. The gain material can overcome the loss of the system by adding supplementary energy, leading to many applications in nanophotonics [23–26]. Notably, graphene, being an atomic-thin material, can be a THz gain medium when an external pump light or electrical bias is applied [26–28]. However, previous literature has provided few reports on the noncontact vacuum friction in gain systems.

In this paper, we unveil the intriguing phenomenon of negative vacuum friction between a rotating nanosphere and a graphene-coated substrate. The friction torque acts as a resistive force in scenarios where the graphene sheet is dominated by loss. However, we demonstrate that negative friction can be achieved by harnessing the THz gain properties of the graphene sheet, particularly at a large quasi-Fermi energy. Also, the dependence of the negative friction on the distance, temperature, and dielectric substrate is investigated. The lower refractive-index substrate is preferred to manifest the negative friction at a low rotation frequency. As the rotation frequency escalates to the THz range, the friction torque exhibits interestingly oscillating spectra, due to the coupling between the localized SPhPs in the nanosphere and the surface modes in the substrate. Our discoveries shed light on a another avenue for driving the rotation of nanoparticles and other related applications.

## II. THEORETICAL MODELS

The proposed system is schematically shown in Fig. 1(a), where a rotating nanosphere with radius $R = 75$ nm is suspended in the vacuum. The separation between the center of the sphere and the substrate is $d$. The substrate is a semi-infinite dielectric plate covered by an active graphene sheet.

*lixinge@hotmail.com

 

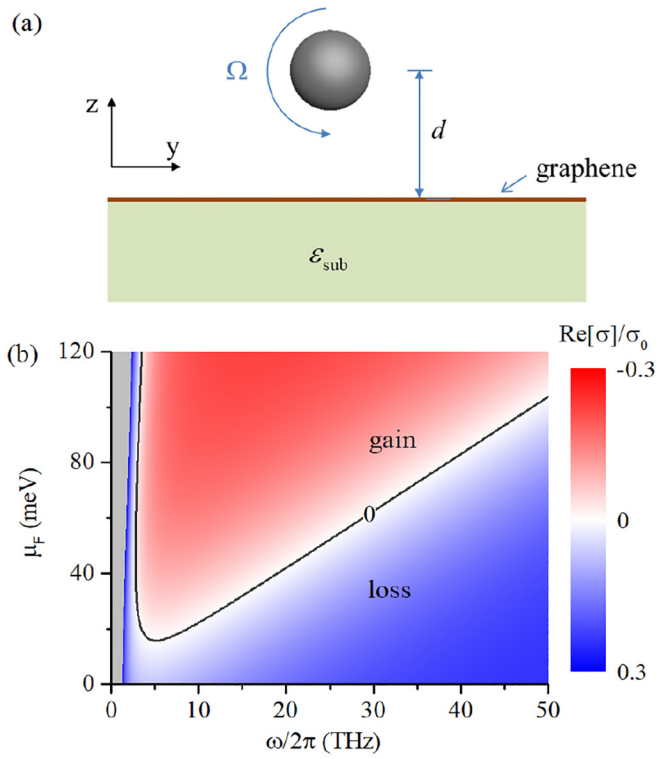


FIG. 1. (a) Schematic view of the system under study. A silica nanosphere with rotational frequency Ω is suspended in the vacuum. The dielectric substrate with permittivity $\epsilon_{\text{sub}}$ is covered by a graphene sheet, which can be a gain medium by applying an external pump light or electrical bias. (b) Contour plot of the real part of graphene conductivity, normalized by $\sigma_0 = e^2/\hbar$. The nanosphere and the substrate is in room temperature with $T_1 = T_2 = 300$ K.

Given that the rotation axis is parallel to the substrate surface, the expression for the frictional torque experienced by the rotating sphere is written as [14]

$$M_p(d) = -\frac{2\hbar}{\pi}\int_{-\infty}^{\infty}[n_1(\omega-\Omega)-n_2(\omega)] \times \text{Im}[\alpha(\omega-\Omega)]\text{Im}[\overline{G}(\omega)]d\omega, \quad (1)$$

where $\hbar$ is the reduced Planck constant, $\omega$ is the angular frequency of the photon, Ω is the angular frequency of the rotating nanosphere, $n_j(\omega) = [\exp(\hbar\omega/k_B T_j) - 1]^{-1}$ is the Bose-Einstein distribution function, $T_j$ $(j = 1, 2)$ is the temperature of the sphere and substrate, $k_B$ is the Boltzmann constant, and $\alpha(\omega) = R^3[\epsilon(\omega) - 1]/[\epsilon(\omega) + 2]$ is the electrical polarization of the nanosphere with $\epsilon(\omega)$ being the permittivity of silica. The Green's function $\overline{G}(\omega)$ is given by

$$\overline{G}(\omega) = \frac{i}{2}\int_0^{\infty} dk_{\parallel}k_{\parallel}e^{2ik_z d}\left[\left(\frac{k_{\parallel}^2}{k_z}-\frac{k_z}{2}\right)r_p + r_s\frac{k_0^2}{2k_z}\right], \quad (2)$$

where $k_{\parallel}$ and $k_z = \sqrt{k_0^2 - k_{\parallel}^2}$ represent the parallel and vertical wave vectors, $k_0 = \omega/c$ is the total wave vector with $c$ being the velocity of light in the vacuum, and $r_s$ and $r_p$ are the reflection coefficients for the polarizations of the transverse electric (TE) and transverse magnetic (TM) modes, respectively. For a graphene-covered substrate, the reflection coefficients can be given analytically as follows [29,30],

$$r_s = \frac{k_{1z} - k_{2z} - k_0\widehat{\sigma}}{k_{1z} + k_{2z} + k_0\widehat{\sigma}}, \quad (3)$$

$$r_p = \frac{\epsilon_1/k_{1z} - \epsilon_2/k_{2z} - \widehat{\sigma}/k_0}{\epsilon_1/k_{1z} + \epsilon_2/k_{2z} + \widehat{\sigma}/k_0}, \quad (4)$$

where $\epsilon_1 = 1$, $\epsilon_2 = \epsilon_{\text{sub}}$, $k_{jz} = \sqrt{\epsilon_j k_0^2 - k_{\parallel}^2}$ $(j = 1, 2)$, $\widehat{\sigma} = \sigma/\eta_0$ represents the normalized graphene conductivity, and $\eta_0$ is the free-space impedance. The conductivity of graphene, as discussed in the Appendix, relies on various parameters including the angular frequency $\omega$, quasi-Fermi energy $\mu_F$, temperature $T$, and relaxation time $\tau$. In this analysis, we adopt a value of $\tau = 1$ ps, which is consistent with recent experimental findings [31]. It is worth noting that the dominant SPP mode in graphene is the TM mode, while the TE mode exhibits relatively weaker characteristics [32]. By equating the denominator of Eq. (4) to zero, we derive the dispersion relation of the SPP for the TM mode.

## III. RESULTS AND DISCUSSIONS

The amplification (gain) or absorption (loss) of SPPs is determined by the real part of the graphene conductivity, as depicted in Fig. 1(b). The negative and positive signs of $\text{Re}[\sigma(\omega)]$ represent the gain and loss of the excited SPPs in graphene, respectively. As anticipated, for small values of the quasi-Fermi energy ($\mu_F$), graphene is predominantly characterized by dissipative losses. However, for $\mu_F$ larger than about 15.8 meV, specific THz bandwidths exhibit a negative conductivity, indicating the presence of gain, and the gain bandwidth enlarges greatly with increasing the quasi-Fermi energy.

The vacuum friction experienced by the rotating nanosphere is linked to the LDOS at its position, which is directly proportional to $\text{Im}[G(\omega)]$ [14,33]. The behavior of $\text{Im}[G(\omega)]$ for a dielectric substrate coated with graphene is depicted in Fig. 2(a), where the separation $d$ is fixed at 300 nm. According to the fluctuation-dissipation theorem, the LDOS should always be positive in a lossy system. For instance, in the case of a bare silica substrate [15], $\text{Im}[G(\omega)]$ is positive across the entire spectrum. However, in our system, the LDOS represented by $\text{Im}[G(\omega)]$ can exhibit both positive and negative values, depending on the magnitude of the quasi-Fermi energy. When graphene functions as a lossy material at a low $\mu_F$, $\text{Im}[G(\omega)]$ is a positive value throughout the spectrum range. Remarkably, as $\mu_F$ surpasses 15.8 meV, $\text{Im}[G(\omega)]$ within the gain bandwidth becomes negative, accompanied by a broadband resonant spectrum. This intriguing negativity of $\text{Im}[G(\omega)]$ within the gain bandwidth opens up the possibility of torque reversal for the rotating sphere.

The enhancement of the LDOS is typically associated with the excitation of hyperbolic modes [12] or surface modes [14,15]. In our system, the resonant behavior observed in $\text{Im}[G(\omega)]$ can be attributed to the SPPs supported by graphene. For $\mu_F = 10$ meV, the SPP corresponds to a lossy surface wave, and the Green's function exhibits positive values across the entire momentum space. The $k$ dependence

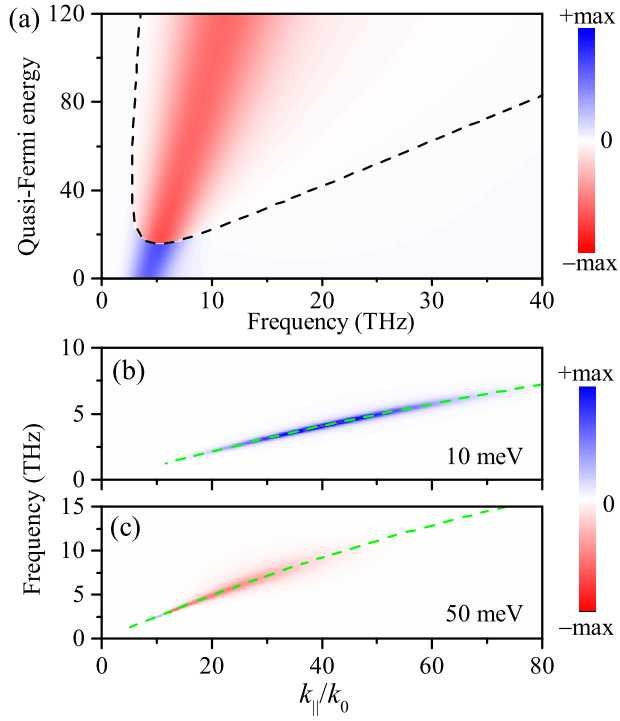


FIG. 2. (a) Im$[G(\omega)]$ for a dielectric substrate $\epsilon_{\text{sub}} = 2$ covered by an active graphene sheet; (b) and (c) represent Im$[G(\omega)]$ contributed by different wave vectors with $\mu_F = 10$ meV and $\mu_F = 50$ meV, respectively. The green dashed lines in (b) and (c) represent the dispersion of SPPs for the TM mode.

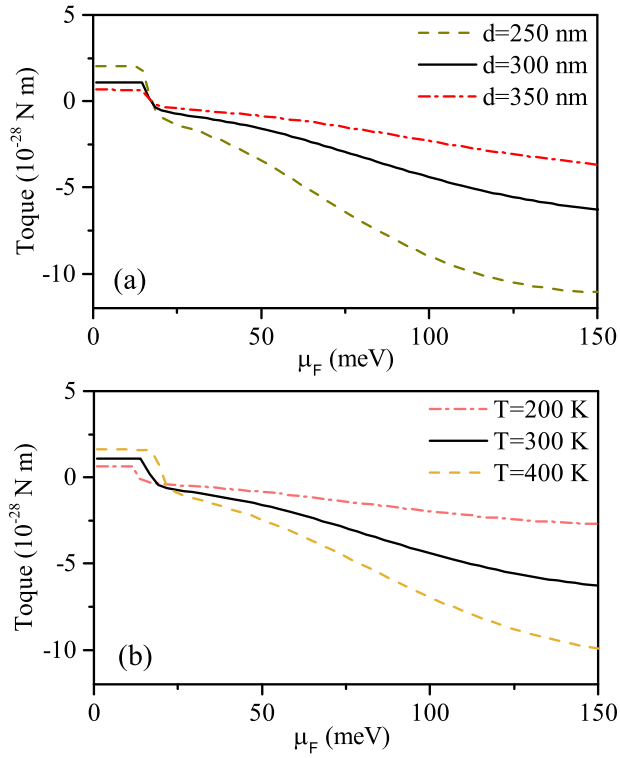


FIG. 3. (a) Friction torque vs quasi-Fermi energy of graphene under different separations, where the temperature $T = 300$ K is fixed. (b) Friction torque vs quasi-Fermi energy of graphene under different temperatures, where the separation $d = 300$ nm is fixed. We set the rotational frequency $\Omega/2\pi = 5$ GHz and $\epsilon_{\text{sub}} = 2$.

of Im$[G(\omega)]$ is consistent with the dispersion relation of the SPP in graphene, as illustrated in Fig. 2(c). Remarkably, as $\mu_F$ increases to 50 meV, the SPP transforms into an amplified surface wave, leading to a negative value of the Green's function [see Fig. 2(c)]. It is important to note that outside the gain bandwidth, Im$[G(\omega)]$ remains positive but is negligibly small.

The variation of the calculated friction torque with respect to $\mu_F$ is shown in Fig. 3(a) for different separations. The nanosphere's rotation frequency is fixed at 5 GHz, which is available in recent experiments [18,19]. Initially, as $\mu_F$ increases from 0 to the critical gain value, the friction torque remains nearly constant and positive. This positive friction exerts a resisting effect, impeding the rotation of the nanosphere. However, as $\mu_F$ continues to increase, the friction torque rapidly decreases and eventually becomes negative, giving rise to a remarkable phenomenon of negative friction. This negative friction creates a positive feedback, driving the nanosphere to higher rotational speeds. Furthermore, the magnitude of the friction is found to be dependent on the separation distance, as indicated by the values of $d = 250$, 300, and 350 nm. Decreasing the separation distance is favored for the manifestation of negative vacuum friction. The role of temperature in the friction torque is also noteworthy, as depicted in Fig. 3(b). The friction torque exhibits an increasing trend with rising the temperature, resembling the conclusions in Ref. [18]. For instance, considering $\mu_F = 100$ meV, the friction torque at $T_1 = T_2 = 400$ K is about four times and two times as large as that at 200 and 300 K, respectively. This demonstrates the significant influence of temperature on the friction torque.

Now we consider the choices of dielectric substrates to realize negative friction torque. The permittivity of the dielectric substrate modulates the SPPs of graphene [30,34], and thus the corresponding LDOS. The friction torque versus different substrates is shown in Fig. 4(a), wherein the rotation frequency is fixed at 5 GHz. Our results suggest that the negative friction manifests greatly with a lower refractive index of the substrate. This is because the decay tail of the SPPs becomes large for a substrate with a lower refractive index, enhancing the LDOS at a fixed separation distance. The friction torque shows quite different features for polar substrates of $SiO_2$ and SiC, due to the presence of SPhPs. Here, the dielectric functions of $SiO_2$ and SiC are described by the Drude-Lorentz mode, given in Ref. [18]. Interestingly, the friction torque is positive for a graphene-covered $SiO_2$ substrate, indicating a resisting effect, while it turns to negative values for the case of SiC, although the magnitude is greatly attenuated. As the rotation frequency increases to 5 THz, the friction torque as a function of quasi-Fermi energy is shown in Fig. 4(b). For large $\mu_F$ (e.g., 100 meV), the friction torque increases by three orders of magnitude compared with the case of 5 GHz. Moreover, a negative torque can be found even for the covered substrate of $SiO_2$.

To uncover the underlying mechanism, Im$[G(\omega)]$ for polar substrates covered by a graphene sheet are shown in Figs. 5(a) and 5(b). The Im$[G(\omega)]$ contributed from the SPPs are relatively broadband and could be negative due to the gain properties at a large $\mu_F$. However, Im$[G(\omega)]$ contributed

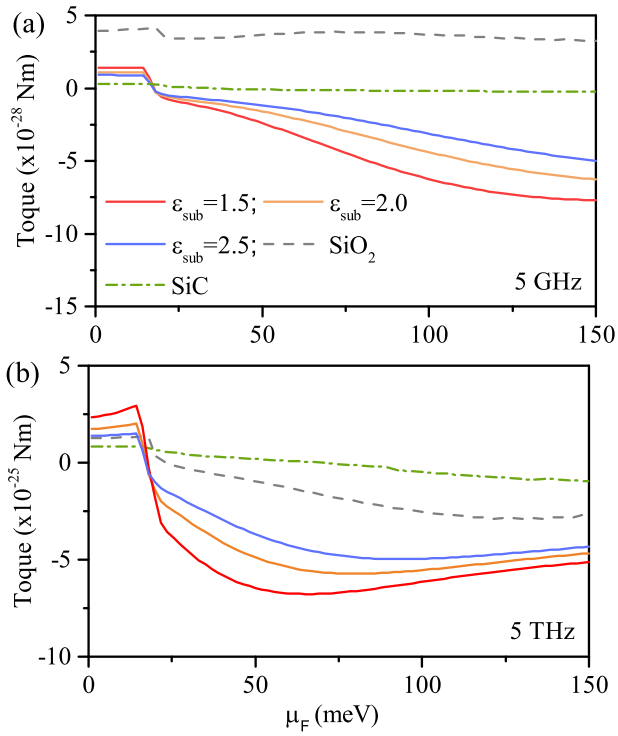


FIG. 4. Friction torque vs quasi-Fermi energy of graphene under different substrates for (a) $\Omega/2\pi = 5$ GHz and (b) $\Omega/2\pi = 5$ THz. Here, we set $d = 300$ nm, $T = 300$ K.

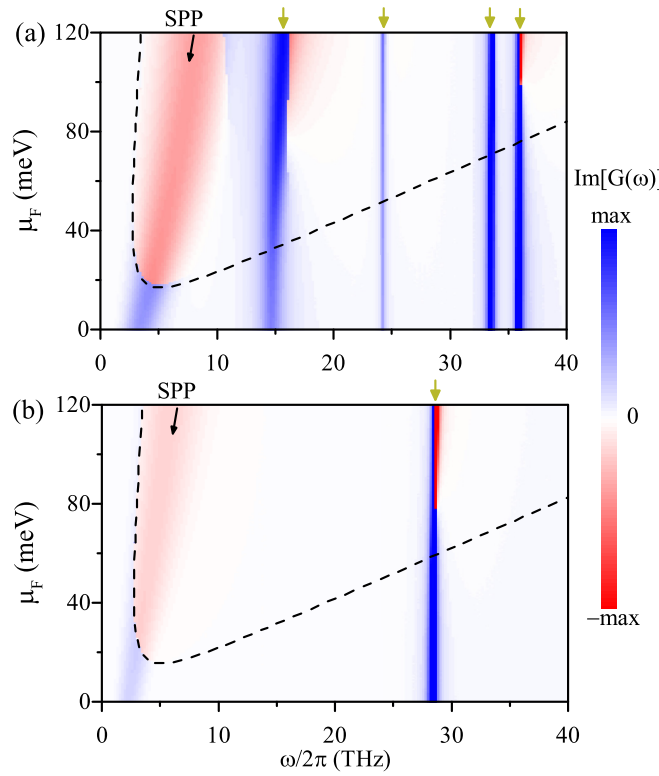


FIG. 5. Im$[G(\omega)]$ for a graphene-covered substrate of (a) $SiO_2$ and (b) SiC. The arrows indicate the resonant exciations of the SPPs in graphene and SPhPs in the polar substrates. The dashed lines represent the gain/loss boundary of graphene.

from the SPhPs are narrowband and mainly positive due to its loss feature. At a low rotation frequency, the localized SPhPs in silica nanosphere couple mainly with the SPhPs of the silica substrate, while their coupling with SPPs in graphene is secondary. Thus, the total friction is positive for graphene-covered $SiO_2$. As the rotational frequency is high [e.g., 5 THz in Fig. 4(b)], the resonance of $\alpha(\omega - \Omega)$ in Eq. (1) is shifted by 5 THz correspondingly. Due to the mismatched resonances, the coupling between localized SPhPs in the nanosphere and SPhPs in the substrate decreases greatly. Hence, the friction torque turns to negative for graphene-covered $SiO_2$ at the THz rotational frequency. Similar discussions could be applied to SiC as well. The resonant frequency of localized SPhPs in the $SiO_2$ nanosphere and SPhPs of SiC is mismatched even at low rotational frequency. The negative friction is attributed to the dominant coupling between the gain SPPs in the substrate and the localized SPhPs in the nanosphere. As a result, the friction torque for a graphene-covered substrate of SiC could be negative for both low and high rotational frequencies.

Figure 6(a) shows the variation of the friction torque $M_p$ as a function of the rotation frequency for different substrates covered by a graphene sheet. The results reveal a proportional relationship between $M_p$ and the rotation frequency within the range from the microwave to the sub-THz regime. For a graphene-covered $SiO_2$ substrate, $M_p$ exhibits a positive value. Conversely, for covered substrates with a dielectric constant of $\epsilon_{sub} = 2$ and SiC, $M_p$ demonstrates a negative behavior across a wide frequency range. In an experimental setup, it is important to consider the air resistance acting on the rotating nanosphere within the vacuum chamber,which is written as [18]

$$M_{air} = \frac{\pi p \Omega (2R)^4}{11.976} \sqrt{\frac{2m_{gas}}{\pi k_B T}}, \tag{5}$$

where $m_{gas} = 4.8 \times 10^{-26}$ kg is the mass of the air molecule, and $p$ represents the air pressure. Clearly, $M_{air}$ is positive and it is proportional to the rotation frequency. Figure 6(a) indicates that the negative friction arising from the substrate with $\epsilon_{sub} = 2$ surpasses the air resistance by approximately fourfold for a pressure of $p = 10^{-10}$ Torr, while the negative friction for the graphene-covered SiC substrate is relatively small, being overshadowed by the air resistance.

The friction torque exhibits oscillating spectra when the rotation is up to the THz level as shown in Fig. 6(b). There are three or four resonance dips for the selected substrates. The oscillation is attributed to the large shifting of the resonance of $\alpha(\omega - \Omega)$, and thereafter the coupling between localized SPhPs in the nanosphere and surface modes in a graphene-covered substrate is modulated by rotation frequency. Interestingly, the friction torque for graphene-covered $SiO_2$ can turn into a negative sign, unlike the case of low frequency in Fig. 6(a). At the resonant frequencies, the magnitudes of the negative friction could be about three times of the air resistance. As for the SiC substrate, the negative vacuum friction experiences a remarkable enhancement compared to low rotation frequencies. It is worth noting that the magnitude

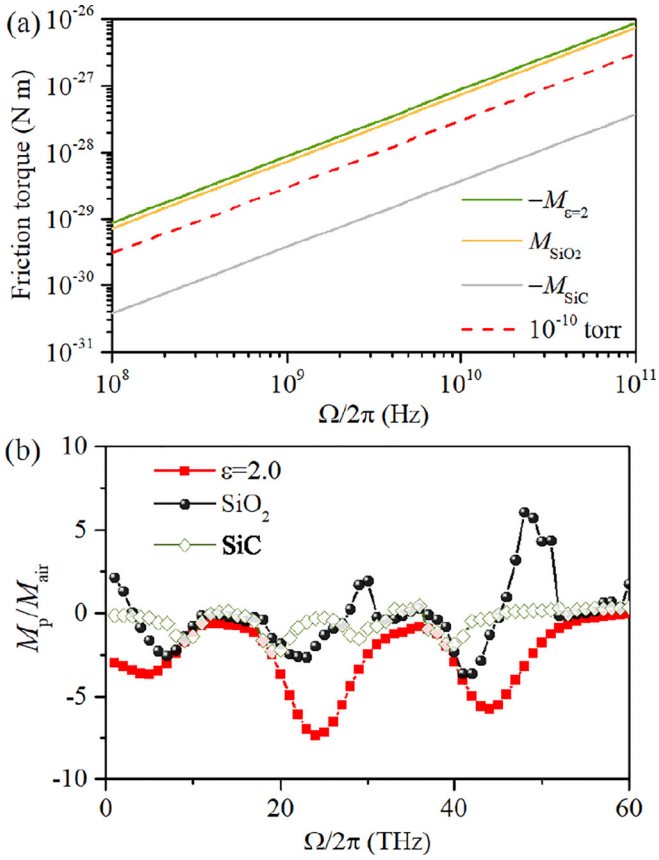


FIG. 6. (a) The friction torque vs the rotational frequency from the microwave to sub-THz regime. The minus sign in the legend represents the negative friction. (b) The contrast of friction torque and air resistance at the THz regime. $\mu_F = 100$ meV.

of the negative torque can be further amplified by decreasing the separation or increasing the temperature [18].

## IV. CONCLUSIONS

In conclusion, this paper unveils the intriguing phenomenon of negative vacuum frictions within a THz gain system, where the direction of friction is along the object's motion. The proposed system comprises a rotating silica nanosphere and a dielectric substrate coated with an active graphene sheet. By manipulating the quasi-Fermi energy of graphene, the sign of the friction torque exerted on the rotating nanosphere can be switched between positive and negative. Negative torque is achieved when the quasi-Fermi energy is large, owing to the remarkable THz gain properties of the graphene sheet. Furthermore, we showcase the dependence of friction magnitude on factors such as distance, temperature, and the dielectric responses of the substrate. We also demonstrate that the torque generated by negative friction surpasses the resistance from the surrounding air across a broad range of rotational frequencies. Our finding provides another avenue for driving the rotation of nanoparticles with ultrafast speed.

## ACKNOWLEDGMENT

This work is supported by the National Natural Science Foundation of China (Grant No. 11804288), and Natural Science Foundation of Henan Province (Grant No. 232300420120).

## APPENDIX: THE CONDUCTIVITY OF AN ACTIVE GRAPHENE SHEET

The graphene sheets shows unique optoelectric properties, due to its gapless Dirac spectrum. The population inversion of charge carriers in a graphene sheet can be obtained under an optical excitation or electrical bias. Then, the graphene conductivity contributed by the intraband and interband transition is written as [35,36]

$$\sigma(\omega) = \frac{e^2}{\hbar}\frac{i2k_BT}{\pi\hbar(\omega+i/\tau)}\ln\left[1+\exp\left(\frac{\mu_F}{k_BT}\right)\right] + \frac{e^2}{4\hbar}\tanh\left(\frac{\hbar\omega-2\mu_F}{4k_BT}\right) + \frac{ie^2\hbar\omega}{\pi\hbar}\int_0^\infty \frac{g(x)-g(\hbar\omega/2)}{(\hbar\omega)^2-4x^2}dx, \quad \text{(A1)}$$

where $\mu_F$ is the quasi-Fermi energy, depending on the strength of the photoexcitation or electrical bias, $e$ is the electron charge, $\tau$ is the momentum relaxation time of charge carriers, the effective temperature $T$ is assumed to be the lattice temperature [36], and

$$g(x) = \frac{\sinh(x/k_BT)}{\cosh(\mu_F/k_BT)+\cosh(x/k_BT)}. \quad \text{(A2)}$$

The interband transition leads to the population inversion, whereas the intraband transition causes the absorption. Fortunately, the graphene conductivity due to the interband transition can prevail over the intraband absorption at a sufficiently strong excitation, resulting in negative Re$[\sigma(\omega)]$.

[1] A. I. Volokitin and B. N. J. Persson, Rev. Mod. Phys. **79**, 1291 (2007).
[2] Q.-D. Jiang and F. Wilczek, Phys. Rev. B **99**, 165402 (2019).
[3] M. B. Farías, F. C. Lombardo, A. Soba, P. I. Villar, and R. S. Decca, npj Quantum Inf. **6**, 25 (2020).
[4] D. Reiche, F. Intravaia, and K. Busch, APL Photonics **7**, 030902 (2022).
[5] J. B. Pendry, J. Phys.: Condens. Matter **9**, 10301 (1997).
[6] A. I. Volokitin and B. N. J. Persson, Phys. Rev. Lett. **106**, 094502 (2011).
[7] M. B. Farias, W. J. M. Kort-Kamp, and D. A. R. Dalvit, Phys. Rev. B **97**, 161407(R) (2018).
[8] R. Luo, J.-R. Yang, T.-B. Wang, D.-J. Zhang, W.-X. Liu, T.-B. Yu, and Q.-H. Liao, Phys. Lett. A **387**, 127006 (2021).
[9] D. Pan, H. Xu, and F. J. García de Abajo, Phys. Rev. Lett. **123**, 066803 (2019).

[10] A. Manjavacas, F. J. Rodríguez-Fortuño, F. J. García de Abajo, and A. V. Zayats, Phys. Rev. Lett. **118**, 133605 (2017).
[11] S. Sanders, W. J. M. Kort-Kamp, D. A. R. Dalvit, and A. Manjavacas, Commun. Phys. **2**, 71 (2019).
[12] T.-B. Wang, Y. Zhou, H.-Q. Mu, K. Shehzad, D.-J. Zhang, W.-X. Liu, T.-B. Yu, and Q.-H. Liao, Nanotechnology **33**, 245001 (2022).
[13] A. Manjavacas and F. J. García de Abajo, Phys. Rev. Lett. **105**, 113601 (2010).
[14] R. Zhao, A. Manjavacas, F. J. García de Abajo, and J. B. Pendry, Phys. Rev. Lett. **109**, 123604 (2012).
[15] Z. Xu, Z. Jacob, and T. Li, Nanophotonics **10**, 537 (2021).
[16] C. Gonzalez-Ballestero, M. Aspelmeyer, L. Novotny, R. Quidant, and O. Romero-Isart, Science **374**, eabg3027 (2021).
[17] B. A. Stickler, K. Hornberger, and M. S. Kim, Nat. Rev. Phys. **3**, 589 (2021).
[18] J. Ahn, Z. Xu, J. Bang, P. Ju, X. Gao, and T. Li, Nat. Nanotechnol. **15**, 89 (2020).
[19] Y. Jin, J. Yan, S. J. Rahman, J. Li, X. Yu, and J. Zhang, Photonics Res. **9**, 1344 (2021).
[20] J. Ahn, Z. Xu, J. Bang, Y.-H. Deng, T. M. Hoang, Q. Han, R.-M. Ma, and T. Li, Phys. Rev. Lett. **121**, 033603 (2018).
[21] R. Reimann, M. Doderer, E. Hebestreit, R. Diehl, M. Frimmer, D. Windey, F. Tebbenjohanns, and L. Novotny, Phys. Rev. Lett. **121**, 033602 (2018).
[22] P. Ju, Y. Jin, K. Shen, Y. Duan, Z. Xu, X. Gao, X. Ni, and T. Li, arXiv:2301.10868.
[23] O. Hess, J. B. Pendry, S. A. Maier, R. F. Oulton, J. M. Hamm, and K. L. Tsakmakidis, Nat. Mater. **11**, 573 (2012).
[24] R. El-Ganainy, K. G. Makris, M. Khajavikhan, Z. H. Musslimani, S. Rotter, and D. N. Christodoulides, Nat. Phys. **14**, 11 (2018).
[25] Y. Fan, N.-H. Shen, F. Zhang, Q. Zhao, Z. Wei, P. Zhang, J. Dong, Q. Fu, H. Li, and C. M. Soukoulis, ACS Photonics **5**, 1612 (2018).
[26] T. Otsuji, V. Popov, and V. Ryzhii, J. Phys. D: Appl. Phys. **47**, 094006 (2014).
[27] D. V. Fateev, O. V. Polischuk, K. V. Mashinsky, I. M. Moiseenko, M. Y. Morozov, and V. V. Popov, Phys. Rev. Appl. **15**, 034043 (2021).
[28] P.-Y. Chen and J. Jung, Phys. Rev. Appl. **5**, 064018 (2016).
[29] O. V. Kotov and Y. E. Lozovik, Phys. Rev. B **96**, 235403 (2017).
[30] T. Zhan, X. Shi, Y. Dai, X. Liu, and J. Zi, J. Phys.: Condens. Matter **25**, 215301 (2013).
[31] I. Gierz, J. C. Petersen, M. Mitrano, C. Cacho, I. Turcu, E. Springate, A. Stöhr, A. Köhler, U. Starke, and A. Cavalleri, Nat. Mater. **12**, 1119 (2013).
[32] S. A. Mikhailov and K. Ziegler, Phys. Rev. Lett. **99**, 016803 (2007).
[33] K. Joulain, R. Carminati, J.-P. Mulet, and J.-J. Greffet, Phys. Rev. B **68**, 245405 (2003).
[34] M. Jablan, H. Buljan, and M. Soljačić, Phys. Rev. B **80**, 245435 (2009).
[35] A. A. Dubinov, V. Y. Aleshkin, V. Mitin, T. Otsuji, and V. Ryzhii, J. Phys.: Condens. Matter **23**, 145302 (2011).
[36] V. V. Popov, O. V. Polischuk, A. R. Davoyan, V. Ryzhii, T. Otsuji, and M. S. Shur, Phys. Rev. B **86**, 195437 (2012).